Nucleic Acids Research, 2005, Vol. 33, No. 8 ***2707–2714***
doi:10.1093/nar/gki568

Nucleoside diphosphate kinase from *Mycobacterium tuberculosis* cleaves single strand DNA within the human *c-myc* promoter in an enzyme-catalyzed reaction

Praveen Kumar, Anjali Verma, Adesh Kumar Saini, Puneet Chopra, Pradip K. Chakraborti[1], Yogendra Singh and Shantanu Chowdhury*

Institute of Genomics and Integrative Biology, CSIR, Mall Road, Delhi 110007, India and [1]Institute of Microbial Technology, Sector 39A, Chandigarh 160036, India

Received March 27, 2005; Revised and Accepted April 21, 2005

ABSTRACT

The reason for secretion of nucleoside diphosphate kinase (NdK), an enzyme involved in maintaining the cellular pool of nucleoside triphosphates in both prokaryotes and eukaryotes, by *Mycobacterium tuberculosis* is intriguing. We recently observed that NdK from *M.tuberculosis* (mNdK) localizes within nuclei of HeLa and COS-1 cells and also nicks chromosomal DNA *in situ* (A. K. Saini, K. Maithal, P. Chand, S. Chowdhury, R. Vohra, A. Goyal, G. P. Dubey, P. Chopra, R. Chandra, A. K. Tyagi, Y. Singh and V. Tandon (2004) *J. Biol. Chem.*, 279, 50142–50149). In the current study, using a molecular beacon approach, we demonstrate that the mNdK catalyzes the cleavage of single strand DNA. It displays Michaelis–Menten kinetics with a k_{cat}/K_M of 9.65 (±0.88) × 10^6 M^{-1} s^{-1}. High affinity ($K_d \approx K_M$ of ~66 nM) and sequence-specific binding to the sense strand of the nuclease hypersensitive region in the *c-myc* promoter was observed. This is the first study demonstrating that the cleavage reaction is also enzyme-catalyzed in addition to the enzymatic kinase activity of multifunctional NdK. Using our approach, we demonstrate that GDP competitively inhibits the nuclease activity with a K_I of ~1.9 mM. Recent evidence implicates mNdK as a potent virulence factor in tuberculosis owing to its DNase-like activity. In this context, our results demonstrate a molecular mechanism that could be the basis for assessing *in situ* DNA damage by secretory mNdK.

INTRODUCTION

Nucleoside diphosphate kinases (NdKs) are essential enzymes that catalyze the reversible transformation of (d)NTPs to (d)NDPs via a covalent phosphohistidine intermediate (1). They play a key role in maintaining the intracellular pool of NTP. NdKs have been characterized from several prokaryotes and eukaryotes and their crystal structures have been determined (1–9). Though they share high homology (43% identity between the *Escherichia coli* and human proteins) the enzymes are tetrameric in most prokaryotes and hexameric in eukaryotes (1,9). In addition to its role in maintaining the NTP pool, several cellular functions have been associated with NdK including cell growth and differentiation in bacteria (2,6) and tumor metastasis suppression in humans (10). In *E.coli*, Ndk has been shown to phosphorylate histidine kinases EnvZ and CheA, implicating its participation in signal transduction systems (6). In *Drosophila melanogaster*, NdK is involved in the development of wing disc cells (11). The human homologs of NdK constitute a family of eight genes (*nm23*-H1–*nm23*-H8), which perform distinct functions depending on their cellular location (12). The most studied members of this family, NM23-H1 and NM23-H2, function as unconventional transcription factors owing to their characteristic DNA binding and cleavage properties (13,14). Both NdKs have been observed to nick the *c-myc* and the PDGF-A promoters, although their biological functions are different (14). NM23-H2 activates transcription of the oncogene *c-myc* (13) while NM23-H1 has been associated with tumor suppression in metastatic melanoma cells (15) and granzyme A induced apoptosis (16).

Interestingly, extracellular secretion of NdK was reported in a number of pathogens including *Pseudomonas aeruginosa* (17), *Trichenella spiralis* (18), *Vibrio cholerae* (19), *Mycobacterium bovis* BCG and *Mycobacterium tuberculosis* (20).

*To whom correspondence should be addressed. Tel: +91 11 2766 6156; Fax: +91 11 2766 7471; Email: shantanuc@igib.res.in

It was proposed that the secreted mycobacterial NdKs could be involved in virulence by ATP-sequestration from macrophage surface-associated P2Z receptors (20). *M.tuberculosis* ($H_{37}Rv$) Ndk (mNdk) was observed to be cytotoxic to mouse macrophage cells, in an ATP-dependent P2Z receptor-mediated pathway (21). Therefore, mNdk may be an important enzyme as a virulence factor in tuberculosis. In this context, we recently reported that green fluorescent protein fused-mNdk expressed within the HeLa and COS 1 cells was detected inside the nuclei of these cells and was also observed to damage chromosomal DNA *in situ* (22). Taking cues from the DNA association property of human NdKs, mNdK was observed to cleave double strand DNA with sequence specificity within the nuclease hypersensitive element (NHE) in the *c-myc* promoter (22). Cleavage required Mg^{2+} and was inhibited in the presence of ATP (22), like NM23-H2 (23).

Guided by these observations, we have taken a closer look at the association of mNdK with single stranded DNA for two reasons. First, NM23-H2 has been reported to bind the single stranded pyrimidine-rich strand within the *c-myc* NHE with >100-fold higher affinity than the double stranded form (24). Second, we observed single-stranded breaks but no oligonucleosomal DNA fragmentation upon incubation of mNdK with isolated nuclei from the HeLa and COS 1 cells (22). The present study extends these observations by demonstrating that mNdK binds the pyrimidine-rich sense strand within the *c-myc* NHE in a sequence-specific manner and induces cleavage within the strand. Using a molecular beacon method we established that the single strand cleavage reaction shows saturation kinetics. The kinetic characterization of this reaction lays the groundwork for assessing *in situ* DNA cleavage by secretory mNdK.

MATERIALS AND METHODS

All chemicals and reagents were purchased from the Sigma Chemical Company (USA). Bacterial culture media were purchased from Difco Laboratories (BBL-Difco, India). mNdK and mutants were expressed as GST fusion protein in *E.coli* using the pGEX-2T expression vector (Pharmacia), and GST-free mNdK was purified after removal of the GST tag (using thrombin) by gel permeation chromatography on a Superdex 200 column as described earlier (22,25). Kinase activity of mNdK was assayed as described earlier (21). Briefly, 1 μg of purified mNdK was incubated with 1 mM (final concentration) of GDP and 10 μCi [γ-^{32}P]ATP (3000 μCi $mmol^{-1}$) along with 0.1 mM ATP in a final volume of 20 μl buffer (50 mM Tris–HCl, 10 mM $MgCl_2$ and 1 mM DTT, pH 7.4). After initiation with addition of ATP, the reaction was stopped after 10 min at room temperature using 2 μl of 10× SDS buffer. One micro liter of the reaction mixture was spotted on a TLC plate and separated using 0.75 M KH_2PO_4 as the moving phase and visualized using autoradiography. The 31mer oligonucleotide P1, d(CCCCACCTTCCCCACCCTCCCCACCCTCCCC) from the promoter site of *c-myc* corresponding to −147 to −117 relative to the transcription initiation site and the corresponding 5′-fluorescein and 3′-tetramethylrhodamine (TAMRA) labeled oligonucleotide FP1T were obtained from Sigma Genosys. Single strand oligonucleotide concentration was determined using molar extinction coefficient ($\varepsilon_{260\,nm}$ = 7913 M^{-1} cm^{-1}) calculated according to Gray (26). Subsequently, P1 was labeled with [γ-^{32}P]ATP in the presence of T4 polynucleotide kinase as described earlier (23).

Circular dichroism of P1 in the presence of mNdK

All CD measurements were performed, as described earlier (27), on Jasco Spectropolarimeter (model J 715) equipped with a thermostat controlled cell holder. CD spectra were recorded from 220 to 350 nm with an averaging time of 3 s. An aliquot of 4.0 μM oligonucleotide (P1) in 50 mM Tris–MES–acetate, pH 6.5, 1 mM $MgCl_2$ and 75 mM NaCl was kept at 37°C for 1 h before titration with increasing mNdK (0.1–0.5 μM, after addition) in the same buffer. Spectra were taken 30 min after each addition.

Determination of equilibrium binding constants by fluorescence spectroscopy

Fluorescence measurements of equilibrium binding constants were made on a Fluoromax 4 (Spex) spectrofluorimeter. The excitation wavelength was 282 nm (slit width, 3 μm) and emission was observed between 300 and 380 nm (slit width, 3 μm). The intrinsic tryptophan fluorescence emission of mNdK (monitored at 340 nm) is quenched on the binding of P1. To determine the equilibrium binding constant, 300 μl of 0.5 μM mNdK in 50 mM Tris–HCl, pH 7.4 containing 1 mM $MgCl_2$ and 75 mM NaCl was equilibrated at 37°C in a quartz fluorescence micro-cuvette before addition of successive aliquots (2–5 μl) of a stock P1 solution prepared in the same buffer. Following each addition the solution was incubated for 30 min prior to fluorescence measurement. Fluorescence decay owing to photobleaching of mNdK in the absence of P1, within the same time, was ∼6% of the total observed in the presence of P1.

The high affinity of P1 for mNdK poses a limitation on the use of the Scatchard analysis that assumes the bound concentration to be very small with respect to the total ligand concentration, which is the case when $K_D \gg E_0$. Under the conditions of our experiment where $K_D \approx E_0$, the data were treated according to a previously published method (28). Briefly, the fractional saturation (y) of the total mNdK binding sites (E_0) was obtained from the ratio of $\Delta F/\Delta F_{max}$, where ΔF_{max} is the limiting value of the difference in fluorescence intensity (ΔF) approached at high concentrations of P1. The concentration of bound ligand (L_b) is related to the concentration of free ligand binding sites (E) and the concentration of free ligand (L) by the law of mass action and the dissociation constant, K_D. Using the relations $L_b = yE_0$ and $L = L_0 - yE_0$, the fractional saturation of the ligand binding sites is related to the total concentration of added ligand, L_0, as given in the following equation:

$$1/(1 - y) = L_o/y(1/K_D) - E_0/K_D. \quad \mathbf{1}$$

A plot of $1/(1 - y)$ versus L_o/y was fitted to a straight line according to the above equation using the experimentally obtained value of ΔF and the known value of E_0 (total hexameric concentration of mNdK) as constraints. The value for the dissociation constant K_D was obtained from the slope of the line, while the intercept gives the stoichiometry of the binding reaction.

DNA cleavage by gel electrophoresis

Radiolabeled P1 (10 nM) was incubated with various concentrations of mNdK (or mNdK mutants) or 0.2 μM mNdK and 2 mM ATP in 50 mM Tris–HCl, pH 7.4, 1 mM (or 20 mM) $MgCl_2$, 75 mM NaCl and 5% glycerol for 10 min at 37°C. All reactions had 1 μM single strand poly(dA) as non-specific competitor. Samples were resolved on 8% native polyacrylamide gel electrophoresis performed in 0.5× TBE buffer at room temperature for 30 min. Gels were vacuum dried and analyzed using a phosphorimager and quantified by IMAGE QUANT software.

Determination of kinetic parameters of enzymatic DNA cleavage using FRET

FRET experiments were performed essentially as described before (29) using a Fluoromax 4 (Spex) spectrofluorimeter with an excitation and emission bandwidth of 2 and 5 nm, respectively, and a 0.2 × 1 cm micro quartz cuvette in a cell holder interfaced with a peltier controlled thermostat. The excitation wavelength was set at 480 nm although absorption maxima of donor is at 492 nm to minimize acceptor absorption and emission spectra were recorded from 500 to 750 nm (30). In a typical experiment 40 nM FP1T (5′-fluorescein and 3′-tetramethylrhodamine (TAMRA) labeled P1) in 300 μl buffer (50 mM Tris-Cl pH 7.4, 1 mM $MgCl_2$, 75 mM NaCl) was first heated at 97°C for 10 min before slowly cooling and equilibrated at 37°C. Following addition of 0.25 nM mNdK (or mNdK mutants) the decay in acceptor emission was monitored at 575 nm. Separate experiments were performed using varying concentration of FP1T (20–400 nM) and the rate of decay in the first 3 min, with or without GDP (0.5 and 1.0 mM) was used to analyze steady state kinetic parameters using Lineweaver–Burk plots. All experiments were repeated at least three times and observed rates were averaged.

RESULTS

mNdK binds to pyrimidine-rich strand within NHE of *c-myc*

The sense strand within the *c-myc* NHE harbors a 31mer cytosine-rich sequence (P1) that adopts an intramolecular C-tetraplex *in vitro* at neutral pH. This secondary structure has a characteristic CD profile (285 and 254 nm as positive and negative maxima respectively; Figure 1a) (27,31). We used this pattern to study the interaction of P1 with mNdK. A concentration dependent decay in both the positive and the negative maxima of the CD spectrum was observed indicating mNdK-induced interaction with the single strand sequence. No change in the CD spectrum was observed in the presence of millimolar concentrations of lysozyme or GST suggesting that the P1–mNdK interaction was specific (27,31). We also observed no change in the CD spectrum on using heat-inactivated mNdK indicating that non-protein contaminants were not responsible for the interaction.

Although the DNA motif is stable under neutral conditions (27) a slightly acidic pH of 6.5 was used to observe the CD characteristics distinctly (Figure 1a). In order to confirm that mNdK was active at this pH we checked the inherent NDP kinase activity of mNdK (Figure 1b, lane 3) where [γ-^{32}P]ATP conversion to radiolabeled GTP (∼94%) was similar to that at pH 7.4 (full conversion, lane 2). In a previous study (27), we established the folding/unfolding dynamics of the C–C^+ intercalated intramolecular DNA motif first observed by Gehring *et al.* (32), where we observed that temperature induced unfolding of the motif led to a decay in the CD peaks. Similarly, the decrease in intensity of the CD spectrum in the presence of mNdK (Figure 1a) may be owing to protein-induced unfolding of the tetraplex motif. However, unlike the temperature-induced unfolding experiment, the positive maxima did not shift to 277 nm (characteristic for the corresponding single strand unstructured form). The CD spectrum was not regained after treatment with proteinase K (or heating denaturing mNdK) consistent with the occurrence of an irreversible change in P1 motif. mNdK-H117A also changed the CD spectrum of P1 irreversibly, however, the lysine mutant K10A did not indicate any appreciable change in the P1 spectrum (data not shown).

Fluorimetric determination of the equilibrium constant

Binding affinity of the P1–mNdK interaction was further probed by monitoring the mNdK fluorescence in the presence of P1. Intrinsic tryptophan fluorescence of mNdK decreased at 348 nm by >50% on titration with P1 (Figure 1c). A plot of the fluorescence intensity at 348 nm versus total concentration of added P1 (Figure 1d) reveals a plateau beyond 400 nM P1. The high affinity of P1 for mNdK precluded the use of the Scatchard analysis that assumes the bound ligand concentration to be very small with respect to the total ligand concentration, which is the case when $K_D \gg E_0$. Under the conditions of our experiment where $K_D \approx E_0$, the data were treated using an alternative equation (28), as described under Materials and Methods. A binding affinity (K_D) of 65.1 ± 6.6 nM and a stoichiometry of ∼1.89 oligonucleotide per protein hexamer were obtained from this analysis, which uses total concentration of added P1 (instead of free P1) and the fractional saturation of active sites ($y = \Delta F/\Delta F_{max}$) (inset, Figure 1d). This is similar to the K_D (85 nM at pH 7.0) obtained with NM23-H2 (human NdK-B) in a previous study in which ∼5% decay of the intrinsic protein fluorescence was monitored (24). In contrast to an earlier study, which concluded that single strand DNA binding was non-specific (24), our observation of significant fluorescence change with P1 but not with a control sequence, dT31, indicated that mNdK binds to P1 in a sequence-specific manner. This was further confirmed by observing quenching owing to P1 (20–420 nM) in the presence of dT31 (5 μM), which also yielded a similar decay profile (and K_D) though the initial protein fluorescence was ∼5% lower in this case. Free P1, even at millimolar concentrations, did not exhibit fluorescence emission between 300 and 600 nm upon excitation at 282 nm. As an additional control for non-specific quenching, the fluorescence of lysozyme was monitored on addition of millimolar concentrations of P1. Less than 1% of the change observed in the presence of mNdK was seen. The binding of P1 to mNdK mutants H117A and K10A were also analyzed using this method. H117A yielded a K_D of 81.3 ± 11.6 nM while K10A affinity was almost 3-fold (212 ± 32.6 nM) less than wild type (data not shown).

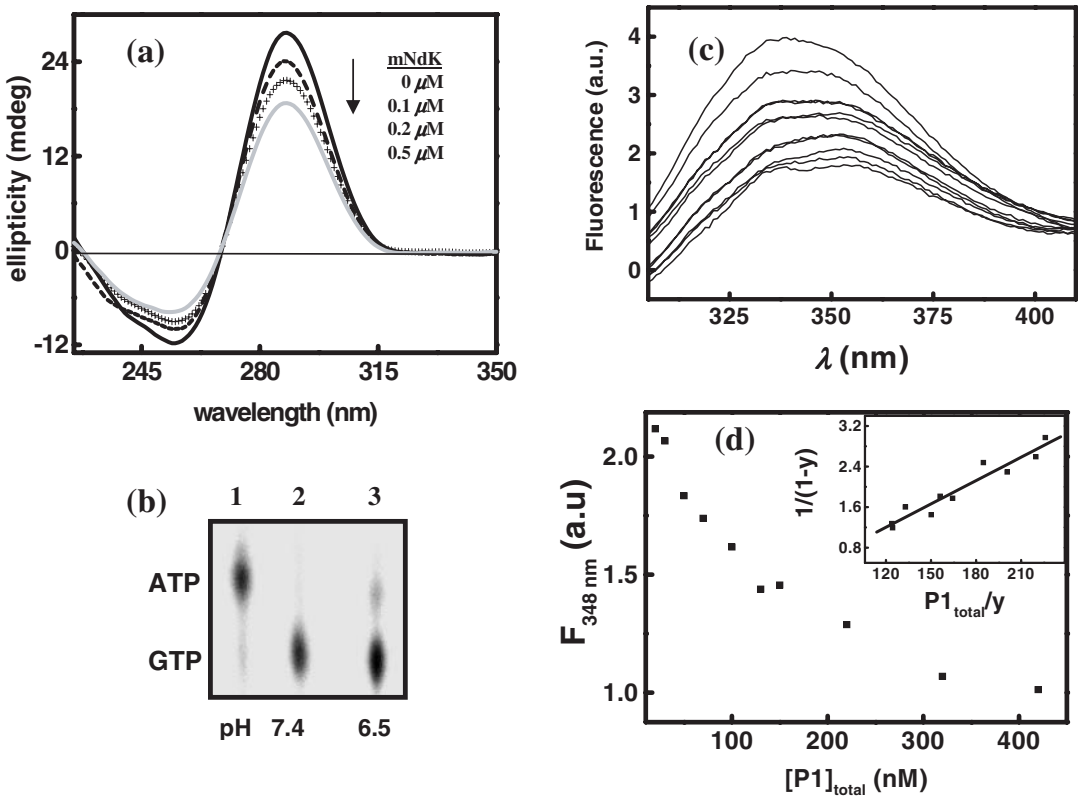

Figure 1. Equilibrium binding of single strand DNA (P1) from *c-myc* promoter with mNdK. CD of folded P1 and decay in intrinsic mNdK fluorescence owing to P1 binding were used to characterize the P1-mNdK interaction. (**a**) mNdK binding disrupts folded P1 motif. CD spectra of P1 (4 μM) shows decrease in ellipticity at 285 nm with increasing mNdK (0–0.5 μM) in 50 mM Tris-MES-acetate pH 6.5, 1 mM $MgCl_2$, 75 mM NaCl within 30 min of incubation, after each addition, at 37°C. (**b**) Enzymatic (phosphotransfer) activity of mNdK at pH 6.5. An aliquot of 10 μCi of [γ-^{32}P]ATP was incubated with either no protein (lane 1) or 1 μM of mNdK at the indicated pH along with 1 mM unlabeled GDP. Experiments were done in 20 μl of 50 mM Tris–HCl, 5 mM $MgCl_2$, 1 mM DTT, pH 7.4 (lanes 1 and 2) or 50 mM Tris–MES–acetate, 5 mM $MgCl_2$, 1 mM DTT, pH 6.5 (lane 3) for 3 min at room temperature. Reactions were stopped with 2 μl 10× SDS buffer and separated using thin layer chromatography (PEI-TLC) in 0.75 M KH_2PO_4 to resolve ATP and GTP. Analysis was done by autoradiography. (**c**) Fluorimetric determination of the equilibrium binding constant for P1 binding to mNdk. mNdK (0.5 μM) was titrated with P1 (20–420 nM) and the intrinsic protein fluorescence owing to tryptophan was monitored in the 300–420 nm range. (**d**) The change in fluorescence at 340 nm was plotted as a function of total P1 concentration. Inset: The fractional saturation, *y*, was plotted versus $[P1]_{total}/y$ according to Equation 1, as described in Materials and Methods. The K_D determined by this method was 65.1 ± 6.6 nM. Fluorescence decay owing to photobleaching within the same time was ∼6%; observed separately without P1. Experiments were done in 50 mM Tris-Cl, pH 7.4 containing 1 mM $MgCl_2$ and 75 mM NaCl at 37°C.

mNdK cleaves cytosine-rich NHE sense strand in the *c-myc* promoter

mNdK-induced sequence-specific double strand cleavage of the *c-myc* NHE was observed in a previous study (22). Incubation of single strand 5′-labeled P1 (10 nM) with mNdK also resulted in a cleaved product (Figure 2a). The amount of cleaved P1 increased as mNdK concentration was increased from 10 nM to 2 μM (lanes 3–7, Figure 2a). A plot of the percentage cleaved product (measured from the relative image intensity of the uncleaved P1 band) versus mNdK concentration clearly shows saturation characteristics (Figure 2b). Non-denaturing electrophoresis conditions were used to detect any protein–oligonucleotide complex formation; however, bands with retarded electrophoretic mobility were not observed. No cleavage was observed in the absence of mNdK (lane 2) or when the non-specific oligonucleotide d(T31) (lane 1) was incubated with 2 mM mNdK. Mutant mNdKs, H117A and K10A were checked for their ability to cleave P1. No difference was observed in the activity of H117A relative to the wild-type mNdk while cleavage was completely abrogated on using K10A (Figure 2c). In accordance with the earlier observations for double strand cleavage (22,23), we observed that the single strand cleavage was also inhibited in the presence of ATP (2 mM; lane 2, Figure 2d) relative to the lane where no ATP was added (lane 1). We also observed that the cleavage reaction required Mg^{2+} (data not shown). Similar conclusions have been made in earlier studies with respect to duplex cleavage (22,23). High Mg^{2+} concentration (20 mM; lane 3) in the presence of 2 mM ATP could not rescue the ATP-dependent inhibition indicating that Mg^{2+} scavenging by ATP does not underlie the observed inhibition and suggests that ATP plays a direct role in inhibiting DNA cleavage. Since mNdK was purified by the removal of the GST-tag from a GST-mNdk fusion protein we checked for cleavage of P1 by pure GST as a control—no cleavage was observed with GST (1–5 μM; Supplementary Figure 1).

mNdk cleaves pyrimidine-rich strand within *c-myc* NHE in an enzyme-catalyzed reaction

We used intramolecularly folded P1 to study its interaction with mNdK by FRET analysis. In a previous study, we have characterized the folding and stability of the cytosine-rich

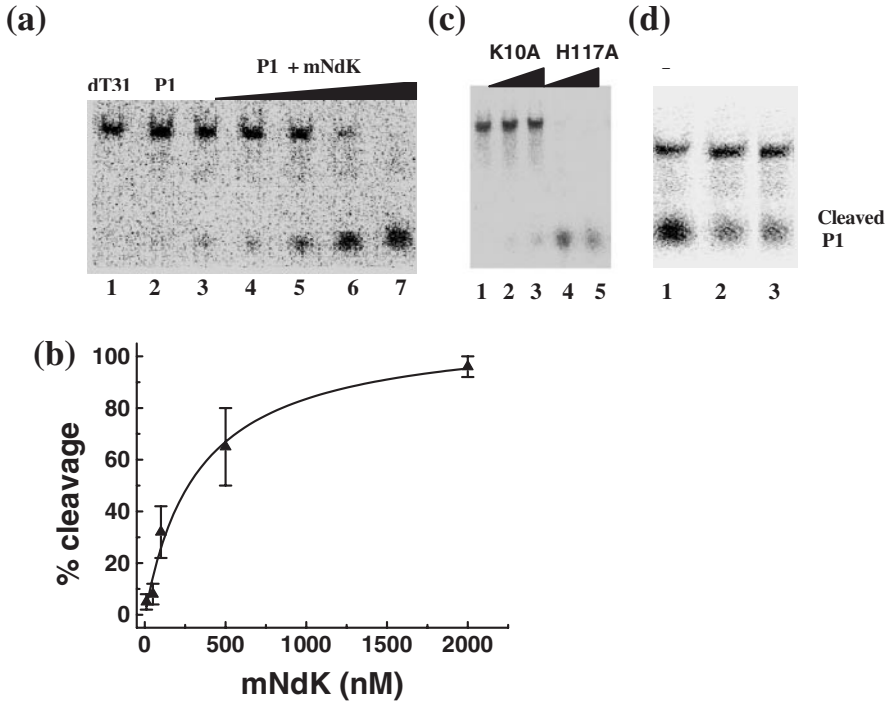

Figure 2. mNdK-induced cleavage of P1 and inhibition of cleavage by ATP. All reactions had 10 nM P1 (or dT31), 5′-end labeled with [γ-^{32}P]ATP. Reactions were performed in 50 mM Tris–HCl, pH 7.4, 1 mM (or 20 mM) $MgCl_2$ and 75 mM NaCl for 10 min at 37°C in the presence of 1 μM single strand poly(dA) as non-specific competitor. (**a**) Autoradiography after separation of cleaved DNA on mNdK treatment. Lane 1,10 nM dT31 in presence of 2 mM mNdK; lanes 2–7, P1 with 0, 10, 50, 100, 500 or 2000 nM mNdk. (**b**) The extent of cleavage in (**a**) is represented as percentage of cleaved P1 versus concentration of mNdK. Amount of cleaved P1 was estimated from image quantification of the uncleaved band. (**c**) P1 cleavage with mNdK mutants. Lane 1, P1 only; lanes 2 and 3, P1 with 1 and 2 μM K10A; lanes 3 and 4, P1 with 1 and 2 μM H117A. (**d**) ATP inhibits mNdK-induced cleavage of P1, which is not abrogated at high Mg^{2+} concentration. All reactions contained P1 and 0.2 μM mNdK. Lane 1, 0 mM ATP; lane 2, 2 mM ATP; lane 3, 2 mM ATP in the presence of 20 mM Mg^{2+}. Cleaved products were separated in a 8% native polyacrylamide gel by electrophoresis in 0.5× TBE buffer at room temperature. Gels were vacuum dried and analyzed using Phosphorimager; image quantification was done using IMAGE QUANT software. Quantification of cleaved product was done from at least three independent experiments.

motif using FRET analysis of the 5′-fluorescein and 3′-TAMRA labeled P1 (FP1T) (29). Temperature induced unfolding in this case resulted in diminished energy transfer. FP1T and P1 gave identical CD spectra indicating that the tetraplex structure was conserved after fluorophore labeling (data not shown). FP1T shows significant energy transfer at 37°C as observed by the acceptor (TAMRA) emission at 575 nm on excitation of the donor (fluorescein) at 480 nm (0 h spectrum in Figure 3a). A mixture of FP1T and mNdK after incubation at 37°C showed loss in energy transfer within 1–18 h as seen by the decay in the acceptor emission (Figure 3a). The FRET signal could not be regained after treatment with proteinase K (gray line, PK in Figure 3a) or heating the solution to 97°C and subsequently cooling to ambient temperature (or 4°C), consistent with the occurrence of an irreversible change in FP1T such as that induced by cleavage. Additionally, heat-inactivated mNdK did not induce any change in FRET ruling out the participation of any non-protein contaminant. The decay in intensity at the emission maxima (575 nm) of the acceptor (TAMRA) suggested an increased Forster's distance between the end labels (30). The rate of loss in energy transfer measured as the decay in emission of TAMRA (at 575 nm) was monitored and plotted as initial steady-state rate (3 min) versus FP1T concentration (inset, Figure 3a). This clearly showed saturation with increasing substrate concentration. A Lineweaver–Burk plot was used to estimate the kinetic parameters (squares, Figure 3b) that are listed in Table 1. The value of K_D estimated from fluorescence quenching (65.1 ± 6.6 nM) and K_M (66.3 ± 6.1 nM) are comparable. Table 1 compares the steady state kinetic parameters for enzymatic phosphotransfer (25) and nuclease activity of mNdK. The observed V_{max}, though lower than that observed for the kinase reaction, is similar to that reported for the enzymatic cleavage of single strand DNA by S1 (6.3×10^{-10} M s^{-1}) and other nucleases (33). It is interesting to note that the K_M for the oligonucleotide was significantly lower than for ATP (23.7 ± 1.4 μM). Overall, the catalytic nuclease activity of mNdK was observed to be more efficient (k_{cat}/K_M) than the kinase reaction (with ATP as substrate). We further studied the effect of GDP on the nuclease activity using the FRET-based approach. As shown in the Lineweaver–Burk plots (Figure 3b), GDP competitively inhibited the nuclease activity to give increased K_M of 89.8 ± 4.7 (circles) and 100.54 ± 5.3 nM (triangles) at 0.5 and 1 mM GDP, respectively. The equilibrium inhibition constant (K_I) for GDP was estimated to be around 1.9 mM. Nuclease activity of mNdK-H117A and K10A, which are deficient in their autophosphorylation/phosphotransfer activity (25), was checked using the kinetic assay. No cleavage of P1 with the K10A mutant was observed. H117A, on the other hand showed nuclease activity very similar to wild-type mNdK (V_{max} = 1.71 (±0.21) × 10^{-10} s^{-1} M; K_M = 65.19 (±7.61) × 10^{-9} M; and k_{cat}/K_M = 7.17 (±1.02) × 10^6 s^{-1} M^{-1}).

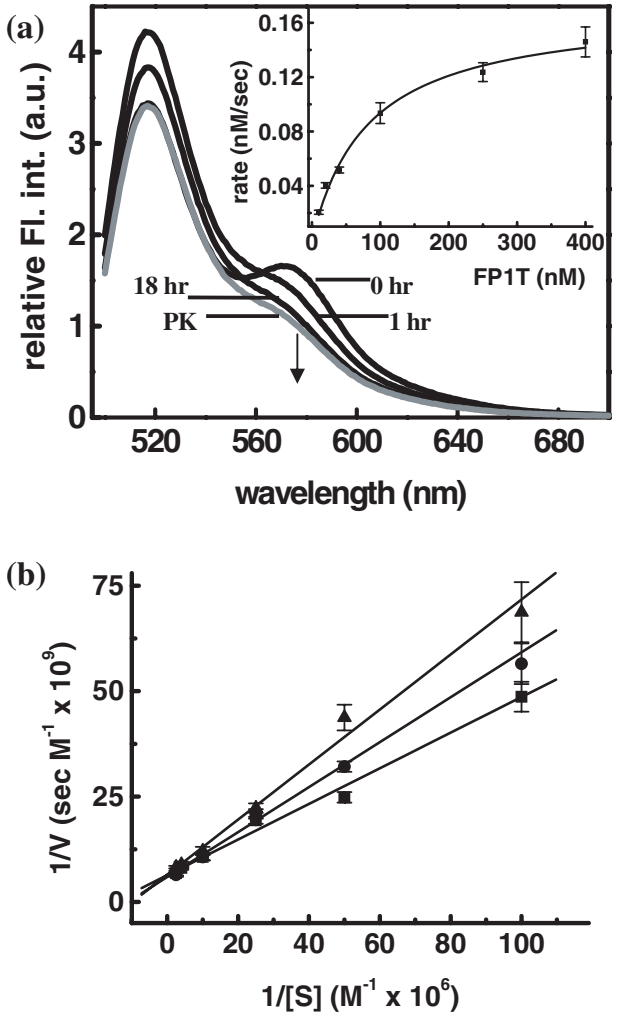

Figure 3. FRET analysis of mNdK-catalyzed cleavage of single strand DNA (FP1T). Decay in FRET of the 5′-fluorescein and 3′-TAMRA labeled pyrimidine-rich single strand from the *c-myc* promoter in the presence of mNdK was analyzed as described in Materials and Methods. (**a**) FRET of the molecular beacon FP1T with mNdK. Spectrum (0 h) showing energy transfer in FP1T emission at 575 nm (acceptor TAMRA) is owing to the energy transfer from donor (fluorescein). Arrow indicates decrease in 575 nm after the specified times (1 and 18 h) following addition of mNdK (0.25 nM) to P1 (40 nM). Grey line (PK) shows spectra of FP1T on treatment with proteinase K (200 μg/ml) after 18 h of incubation with mNdK. Inset: initial (3 min) rate of decay at 575 nm with varying concentration of FP1T (20–400 nM) and 0.25 nM mNdK. (**b**) Lineweaver–Burk plots of the cleavage reaction of FP1T (20–400 nM) by mNdK (0.25 nM) with 0 mM (squares), 0.5 mM (circles) or 1 mM (triangles) of added GDP. FRET was observed, in all cases, on excitation at 480 nm. All experiments were done in 50 mM Tris–HCl, pH 7.4 containing 1 mM $MgCl_2$ and 75 mM NaCl at 37°C and values are averaged from at least three independent experiments.

DISCUSSION

Results obtained in this study suggest that DNA-damage by mNdK within the *c-myc* NHE is induced by sequence-specific single strand DNA binding, followed by enzyme-catalyzed cleavage. Our previous results suggested that nicking of host cell DNA by mNdK occurred at multiple sites and was not specific to the *c-myc* NHE (22). This is consistent with the observation that NM23 proteins target at least two promoter elements in *PDGF-A* and five different genes involved in myeloid-specific differentiation (*myeloperoxidase*, *CCR5*, *CD11b*, *CD11c* and *CD54*) besides *c-myc* (14,34). Additionally, NM23-H1 was recently reported as the DNase involved in single strand nicking during granzyme-A mediated apoptosis (16). Interestingly, these activities have been related to the non-B-form regions of DNA (14). However, mNdK is not a non-specific DNase as indicated by several lines of evidence. It does not bind or cleave a 31mer dT oligonucleotide, nor does it cleave a 45mer double strand ATGC repeat sequence or plasmids without the *c-myc* NHE insert (pUC19 and pGEX-5X3) (22). Herein, in order to characterize the mNdK induced single strand cleavage and its binding with non-B-form DNA we selected the *c-myc* NHE site because of the following reasons. (i) DNA cleavage by NM23-H2 (human NdK) at the *c-myc* site has already been characterized [though this was not observed to be enzyme-catalyzed and single strand cleavage was not studied (24)]. (ii) Several reports have speculated that the interaction could be induced by the DNA secondary structure formation at the NHE site, however, there is no direct evidence for this (14,24,31,35). With respect to (i) the pyrimidine-rich coding strand was selected as several studies on *c-myc* regulation suggest that NM23-H2 (human NdK-B) exerts its functional role by binding to this strand in the *c-myc* promoter (24,31,35). Our results addressing (ii) show mNdK concentration-dependent decay in the CD spectrum of the pyrimidine rich motif (Figure 1a) indicating that mNdk changed the topology of the tetraplex fold.

Table 1. Kinetic parameters of nuclease and kinase activity exhibited by mNdK

	V_{max} (s^{-1} M)	K (M)	k_{cat}/K_M (s^{-1} M^{-1})
Nuclease activity	1.62 (±0.16) × 10^{-10}	66.32 (±6.14) × 10^{-9}	9.65 (±0.88) × 10^6
Kinase activity	2.83 (±0.49) × 10^{-7}	23.70 (±1.40) × 10^{-6}	2.03 (±0.43) × 10^5

Nuclease assays were performed using FRET as described in Materials and Methods. Different concentrations of substrate FP1T (20–400 nM) was equilibrated in buffer before adding mNdK (0.25 nM/reaction) and monitoring the initial rate of FRET decay. K_M and V_{max} values were estimated from Lineweaver–Burk plot (Figure 3b) and the results are expressed as mean ± SD of at least three independent experiments. The kinetic parameters for the kinase activity (with ATP as substrate) are from Ref. (26).

mNdK has a single tryptophan moiety (Trp132) that is harbored within the nucleotide binding site as observed in the crystal structure of the GDP-bound enzyme (36). This was exploited for determining the equilibrium binding parameters and sequence specificity of the P1–mNdK interaction using the decay in intrinsic tryptophan fluorescence of mNdK. Our results are in contrast to those from an earlier study, using a similar method (and NM23-H2), on two aspects (24). We observed (i) relatively large (∼50%) decay in mNdk fluorescence versus NM23-H2 (∼5%) and (ii) that the interaction was sequence specific while NM23-H2 was reported to be non-specific. A possible reason for the discrepancy could be that instead of one Trp132 in mNdk, NM23-H2 has three tryptophan residues (Trp78, 133, 149); their respective locations are depicted in Figure 4 (12,37). The reduced decay of intrinsic protein fluorescence in NM23-H2 could be owing to a cumulative response of opposing fluorescence changes in the three residues. Moreover, the location of Trp78 and Trp149 outside

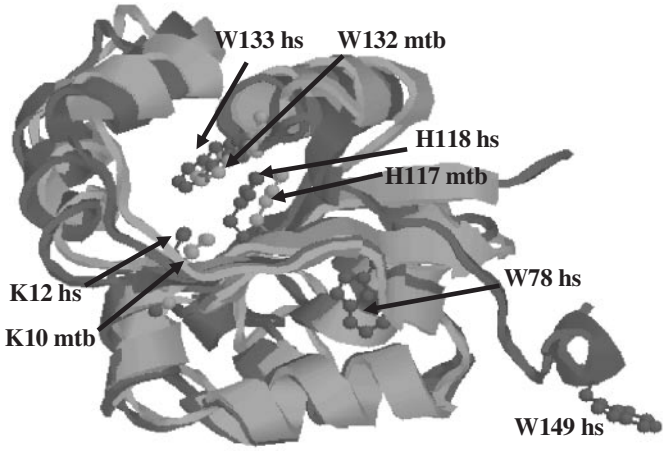

Figure 4. Comparison of NM23-H2 (human NdK-B) and (mNdK) structures. Superimposed ribbon diagrams of mNdK (light colored) and NM23-H2 (dark colored) monomers showing the critical residues (labeled as hs for human and mtb for *M.tuberculosis*)—Lys and His for DNA cleavage and phosphotransfer activity, respectively, in the nucleotide binding pocket. Respective tryptophan residues, one for *M.tuberculosis* and three for human are also shown. This figure was generated using Swiss-pdb viewer (41) with PDB files: 1K44 (mNdK) and 1NSK (NM23-H2).

the active site may result in non-specific changes in the presence of the oligonucleotide.

A similar method, i.e. kinetic analysis using FRET of molecular beacons, has been reported previously for S1 and other nucleases (33). It is important to point out that our assay does not distinguish between DNA binding versus cleavage, as binding could result in DNA conformational changes leading to fluorescence decay. We have three reasons to believe that the fluorescence decay observed in this study is owing to enzymatic DNA cleavage. First, we confirmed DNA cleavage under steady-state conditions using gel electrophoresis. Second, we confirmed DNA cleavage *in situ* (at different time points) by denaturing the enzyme and allowing the substrate to reform the DNA motif; only a fraction of the original fluorescence (depending on the time point) was regained suggesting that the rest of the substrate molecules had been irreversibly changed. Third, even at high substrate versus protein molar ratios we observed full decay of the acceptor fluorescence. This would not be observed if fluorescence decay was owing to protein binding since only a fraction of the molecules would be bound by mNdK.

Unlike other tetrameric bacterial NdKs *mycobacterium*-NdK is hexameric like eukaryotic NdKs (36). It shares close sequence (except the C-terminal residues 138–152 in NM23-H2, which are absent in mNdK) and structural homology with NM23-H2, specially in the DNA binding domain where the critical residues required for DNA binding and cleavage are conserved (Figure 4) (36). Several studies have reported that the residues required for DNA binding are located on the exposed equatorial surface of the hexamer while the residue essential for cleavage (Lys12 in Nm23-H2 and Lys10 in mNdK) is buried inside the active site cleft (38,39). This suggests that the protein may undergo reorganization for nuclease activity. The requirement of substantial conformational changes for catalysis may be the reason for low V_{max}, though K_M for the oligonucleotide binding is low. Interestingly, GDP competitively inhibited the nuclease reaction with a K_I (~1.9 mM) that is somewhat more than the reported K_M of NDPs (0.25–0.5 mM) in relation to the kinase activity (1). Herein, we used GDP to demonstrate that our approach could be used to quantitatively assess the effect of various factors vis-à-vis DNA cleavage by mNdK.

The multiple biochemical functions observed for NM23-H2, including duplex DNA cleavage and NDP kinase activity, and the fact that the critical residues required for these functions share the same active site raises an obvious question—are the activities interdependent? Several studies have addressed this issue with NM23-H2 primarily owing to its implications for *c-myc* transcriptional activation (38–40). In order to check the interrelationship between the kinase and nuclease activities of mNdK we selected two mutants, H117A and K10A, wherein the critical residues for kinase and nuclease functions, respectively, were substituted. mNdK-H117A lacks autophosphorylation/phosphotransfer activity and K10A lacks phosphotransfer activity [while retaining very low (~10%) autophosphorylation activity] (25). Our results indicated that the H117A mutant is very similar to wild-type mNdK vis-à-vis its DNA binding and nuclease activity while as expected the nuclease activity was completely abolished in K10A (Figure 2c). Interestingly, the DNA binding affinity of K10A decreased only 3-fold. The above observations are consistent with previous findings using NM23-H2 mutants and double strand DNA from the *c-myc* NHE (38) and suggest that Lysine 12 is important for both the biochemical functions of mNdk whereas the histidine residue critical for phosphotransfer appears to play no role in the nuclease activity.

The nuclease activity and nuclear localization of mNdK suggest that mNdK can be a potent virulence factor in tuberculosis (22). Though the DNase activity is important for the bacterial dissemination this could be detrimental to the initial growth of the pathogen inside the host cell. One of the possibilities for inhibition of the nuclease reaction is by ATP (Figure 2a). Interestingly, in the context of granzyme-A mediated apoptosis, the DNase activity of NM23-H1 was inhibited by complex formation with the nucleosome assembly protein (SET) components. Following degradation of SET, NM23-H1 nicks chromosomal DNA inducing apoptosis (16). It can be conjectured here that ATP sequestration and/or complex formation with other intracellular components may be necessary to abrogate/control the cleavage activity till an appropriate signaling mechanism activates DNase activity. In this respect, our findings characterizing the molecular mechanism of DNA damage supports the *in vivo* infection model and is likely to augment further search for molecules, which abrogate mNdK mediated DNase activity.

SUPPLEMENTARY MATERIAL

Supplementary Material is available at NAR Online.

ACKNOWLEDGEMENTS

S.C. and Y.S. acknowledge Prof. Samir K. Brahmachari for constant support and CSIR for funding this research. P.K., A.V. and A.K.S. acknowledge research fellowship from CSIR. We thank Souvik Maiti and other members of our group for many helpful discussions and Ruma Banerjee,

UNL, USA for carefully editing the manuscript. The Open Access publication charges for this article have been waived by Oxford University Press.

Conflict of interest statement. None declared.

REFERENCES

1. Lascu,I. and Gonin,P. (2000) The catalytic mechanism of nucleoside diphosphate kinases. *J. Bioenerg. Biomembr.*, **32**, 237–246.
2. Munoz-Dorado,J., Inouye,S. and Inouye,M. (1990) Nucleoside diphosphate kinase from Myxococcus xanthus. II. Biochemical characterization. *J. Biol. Chem.*, **265**, 2707–2712.
3. Lacombe,M.L., Wallet,V., Troll,H. and Veron,M. (1990) Functional cloning of a nucleoside diphosphate kinase from Dictyostelium discoideum. *J. Biol. Chem.*, **265**, 10012–10018.
4. Hama,H., Almaula,N., Lerner,C.G., Inouye,S. and Inouye,M. (1991) Nucleoside diphosphate kinase from *Escherichia coli*; its overproduction and sequence comparison with eukaryotic enzymes. *Gene*, **105**, 31–36.
5. Hildebrandt,M., Lacombe,M.L., Mesnildrey,S. and Veron,M. (1995) A human NDP-kinase B specifically binds single-stranded poly-pyrimidine sequences. *Nucleic Acids Res.*, **23**, 3858–3864.
6. Sundin,G.W., Shankar,S., Chugani,S.A., Chopade,B.A., Kavanaugh-Black,A. and Chakrabarty,A.M. (1996) Nucleoside diphosphate kinase from Pseudomonas aeruginosa: characterization of the gene and its role in cellular growth and exopolysaccharide alginate synthesis. *Mol. Microbiol.*, **20**, 965–979.
7. Lacombe,M.L., Milon,L., Munier,A., Mehus,J.G. and Lambeth,D.O. (2000) The human Nm23/nucleoside diphosphate kinases. *J. Bioenerg. Biomembr.*, **32**, 247–258.
8. Postel,E.H. and Abramczyk,B.M. (2003) *Escherichia coli* nucleoside diphosphate kinase is a uracil-processing DNA repair nuclease. *Proc. Natl Acad. Sci. USA*, **100**, 13247–13252.
9. Janin,J., Dumas,C., Morera,S., Xu,Y., Meyer,P., Chiadmi,M. and Cherfils,J. (2000) Three-dimensional structure of nucleoside diphosphate kinase. *J. Bioenerg. Biomembr.*, **32**, 215–225.
10. Steeg,P.S., Bevilacqua,G., Kopper,L., Thorgeirsson,U.P., Talmadge,J.E., Liotta,L.A. and Sobel,M.E. (1988) Evidence for a novel gene associated with low tumor metastatic potential. *J. Natl Cancer Inst.*, **80**, 200–204.
11. Biggs,J., Hersperger,E., Steeg,P.S., Liotta,L.A. and Shearn,A. (1990) A Drosophila gene that is homologous to a mammalian gene associated with tumor metastasis codes for a nucleoside diphosphate kinase. *Cell*, **63**, 933–940.
12. Morera,S., Lacombe,M.L., Xu,Y., LeBras,G. and Janin,J. (1995) X-ray structure of human nucleoside diphosphate kinase B complexed with GDP at 2 Å resolution. *Structure*, **3**, 1307–1314.
13. Postel,E.H., Berberich,S.J., Flint,S.J. and Ferrone,C.A. (1993) Human c-myc transcription factor PuF identified as nm23-H2 nucleoside diphosphate kinase, a candidate suppressor of tumor metastasis. *Science*, **261**, 478–480.
14. Ma,D., Xing,Z., Liu,B., Pedigo,N.G., Zimmer,S.G., Bai,Z., Postel,E.H. and Kaetzel,D.M. (2002) NM23-H1 and NM23-H2 repress transcriptional activities of nuclease-hypersensitive elements in the platelet-derived growth factor-A promoter. *J. Biol. Chem.*, **277**, 1560–1567.
15. Lacombe,M.L., Sastre-Garau,X., Lascu,I., Vonica,A., Wallet,V., Thiery,J.P. and Veron,M. (1991) Overexpression of nucleoside diphosphate kinase (Nm23) in solid tumours. *Eur. J. Cancer*, **27**, 1302–1307.
16. Fan,Z., Beresford,P.J., Oh,D.Y., Zhang,D. and Lieberman,J. (2003) Tumor suppressor NM23-H1 is a granzyme A-activated DNase during CTL-mediated apoptosis, and the nucleosome assembly protein SET is its inhibitor. *Cell*, **112**, 659–672.
17. Shankar,S., Kamath,S. and Chakrabarty,A.M. (1996) Two forms of the nucleoside diphosphate kinase of Pseudomonas aeruginosa 8830: altered specificity of nucleoside triphosphate synthesis by the cell membrane-associated form of the truncated enzyme. *J. Bacteriol.*, **178**, 1777–1781.
18. Gounaris,K., Thomas,S., Najarro,P. and Selkirk,M.E. (2001) Secreted variant of nucleoside diphosphate kinase from the intracellular parasitic nematode Trichinella spiralis. *Infect. Immun.*, **69**, 3658–3662.
19. Punj,V., Zaborina,O., Dhiman,N., Falzari,K., Bagdasarian,M. and Chakrabarty,A.M. (2000) Phagocytic cell killing mediated by secreted cytotoxic factors of Vibrio cholerae. *Infect. Immun.*, **68**, 4930–4937.
20. Zaborina,O., Li,X., Cheng,G., Kapatral,V. and Chakrabarty,A.M. (1999) Secretion of ATP-utilizing enzymes, nucleoside diphosphate kinase and ATPase, by *Mycobacterium bovis* BCG: sequestration of ATP from macrophage P2Z receptors? *Mol. Microbiol.*, **31**, 1333–1343.
21. Chopra,P., Singh,A., Koul,A., Ramachandran,S., Drlica,K., Tyagi,A.K. and Singh,Y. (2003) Cytotoxic activity of nucleoside diphosphate kinase secreted from *Mycobacterium tuberculosis*. *Eur. J. Biochem.*, **270**, 625–634.
22. Saini,A.K., Maithal,K., Chand,P., Chowdhury,S., Vohra,R., Goyal,A., Dubey,G.P., Chopra,P., Chandra,R., Tyagi,A.K. *et al.* (2004) Nuclear localization and *in situ* DNA damage by Mycobacterium tuberculosis nucleoside-diphosphate kinase. *J. Biol. Chem.*, **279**, 50142–50149.
23. Postel,E.H. (1999) Cleavage of DNA by human NM23-H2/nucleoside diphosphate kinase involves formation of a covalent protein-DNA complex. *J. Biol. Chem.*, **274**, 22821–22829.
24. Agou,F., Raveh,S., Mesnildrey,S. and Veron,M. (1999) Single strand DNA specificity analysis of human nucleoside diphosphate kinase B. *J. Biol. Chem.*, **274**, 19630–19638.
25. Tiwari,S., Kishan,K.V., Chakrabarti,T. and Chakraborti,P.K. (2004) Amino acid residues involved in autophosphorylation and phosphotransfer activities are distinct in nucleoside diphosphate kinase from Mycobacterium tuberculosis. *J. Biol. Chem.*, **279**, 43595–43603.
26. Gray,D.M., Hung,S.H. and Johnson,K.H. (1995) Absorption and circular dichroism spectroscopy of nucleic acid duplexes and triplexes. *Meth. Enzymol.*, **246**, 19–34.
27. Mathur,V., Verma,A., Maiti,S. and Chowdhury,S. (2004) Thermodynamics of i-tetraplex formation in the nuclease hypersensitive element of human c-myc promoter. *Biochem. Biophys. Res. Commun.*, **320**, 1220–1227.
28. Stinson,R.A. and Holbrook,J.J. (1973) Equilibrium binding of nicotinamide nucleotides to lactate dehydrogenases. *Biochem. J.*, **131**, 719–728.
29. Kumar,P., Kajal,K., Gargallo,R. and Chowdhury,S. (2005) Application of Multivariate Curve Resolution for the study of folding processes of DNA monitored by Fluorescence Resonance Energy Transfer. *Anal. Chim. Acta.*, **536**, 135–143.
30. Mergny,J.L. (1999) Fluorescence energy transfer as a probe for tetraplex formation: the i-motif. *Biochemistry*, **38**, 1573–1581.
31. Simonsson,T., Pribylova,M. and Vorlickova,M. (2000) A nuclease hypersensitive element in the human c-myc promoter adopts several distinct i-tetraplex structures. *Biochem. Biophys. Res. Commun.*, **278**, 158–166.
32. Gehring,K., Leroy,J.L. and Gueron,M. (1993) A tetrameric DNA structure with protonated cytosine.cytosine base pairs. *Nature*, **363**, 561–565.
33. Li,J.J., Geyer,R. and Tan,W. (2000) Using molecular beacons as a sensitive fluorescence assay for enzymatic cleavage of single-stranded DNA. *Nucleic Acids Res.*, **28**, E52.
34. Postel,E.H., Berberich,S.J., Rooney,J.W. and Kaetzel,D.M. (2000) Human NM23/nucleoside diphosphate kinase regulates gene expression through DNA binding to nuclease-hypersensitive transcriptional elements. *J. Bioenerg. Biomembr.*, **32**, 277–284.
35. Siddiqui-Jain,A., Grand,C.L., Bearss,D.J. and Hurley,L.H. (2002) Direct evidence for a G-quadruplex in a promoter region and its targeting with a small molecule to repress c-MYC transcription. *Proc. Natl Acad. Sci. USA*, **99**, 11593–11598.
36. Chen,Y., Morera,S., Mocan,J., Lascu,I. and Janin,J. (2002) X-ray structure of Mycobacterium tuberculosis nucleoside diphosphate kinase. *Proteins*, **47**, 556–557.
37. Webb,P.A., Perisic,O., Mendola,C.E., Backer,J.M. and Williams,R.L. (1995) The crystal structure of a human nucleoside diphosphate kinase, NM23-H2. *J. Mol. Biol.*, **251**, 574–587.
38. Postel,E.H., Abramczyk,B.A., Gursky,S.K. and Xu,Y. (2002) Structure-based mutational and functional analysis identify human NM23-H2 as a multifunctional enzyme. *Biochemistry*, **41**, 6330–6337.
39. Postel,E.H., Abramczyk,B.M., Levit,M.N. and Kyin,S. (2000) Catalysis of DNA cleavage and nucleoside triphosphate synthesis by NM23-H2/NDP kinase share an active site that implies a DNA repair function. *Proc. Natl Acad. Sci. USA*, **97**, 14194–14199.
40. Postel,E.H. and Ferrone,C.A. (1994) Nucleoside diphosphate kinase enzyme activity of NM23-H2/PuF is not required for its DNA binding and *in vitro* transcriptional functions. *J. Biol. Chem.*, **269**, 8627–8630.
41. Guex,N. and Peitsch,M.C. (1997) SWISS-MODEL and the Swiss-PdbViewer: an environment for comparative protein modeling. *Electrophoresis*, **18**, 2714–2723.